X-ray optics for axion helioscopes

Anders C. Jakobsen[a], Michael J. Pivovaroff[b] and Finn E. Christensen[a]

[a]Danish Technical University (DTU) Space, Elektrovej 327, DK-2800 Kgs. Lyngby, Denmark
[b]Lawrence Livermore National Laboratory, 7000 East Avenue, Livermore, CA 94550, USA

ABSTRACT

A method of optimizing grazing incidence x-ray coatings in ground based axion helioscopes is presented. Software has been been developed to find the optimum coating when taking both axion spectrum and Micromegas detector quantum efficiency into account. A comparison of the relative effective area in the telescope using different multilayer material combinations is produced. Similar methods are used for IAXO, a planned axion helioscope. Additionally, the optimal focal length is modelled while taking into account the least possible background contribution from the detector.

Keywords: X-ray optics, axion, multilayer coatings

1. INTRODUCTION

Axions are theoretical particles created by the Primakoff effect[1] from photons interacting with strong electric and magnetic fields. An obvious place to look for axions would then be our own sun. The particles are weakly interacting, so detection becomes a challenge. A solution is to use the Primakoff effect again to reconvert the axion into a photon using a strong magnetic field and subsequently detecting the photon in an x-ray detector as seen in figure 1.

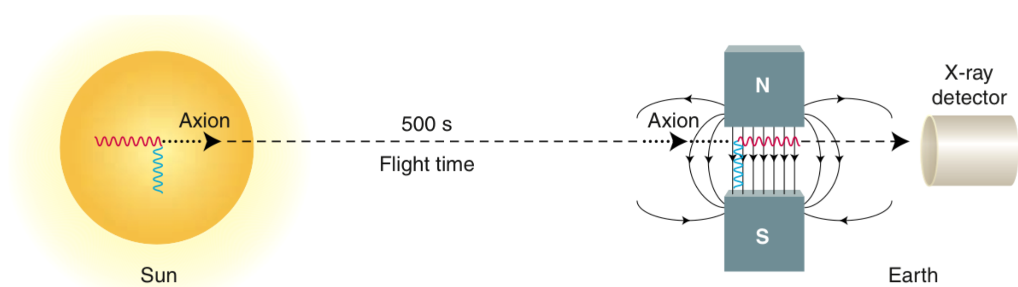

Figure 1. Diagram of axions created by the Primakoff effect in the sun, travelling to Earth and getting detected using a strong magnetic field and a detector.

In the past 30 years the hunt for axions as a solution to CP violation in particle physics and a possible candidate for dark matter, have required larger and more sensitive instruments. The third and latest generation of helioscopes for axion detection is the CERN Axion Solar Telescope (CAST),[2–5] consisting of a LHC prototype magnet and low background MicroMegas detectors.[6]

The main problem is to distinguish a small signal amidst the background, which largely comes from the detector. The magnetic bores on CAST are 50 mm wide, so a detector to cover a bore consequently becomes large. The detector area is proportional to the background squared. A solution is to reflect the x-ray photons coming from the bore in an x-ray optic and onto a much smaller detector. In the next section, the design of such an optic is explained.

Further author information:
A.C.J.: E-mail: jakobsen@space.dtu.dk, Telephone: +45 4525 9735

2. CAST TELESCOPE GEOMETRY

The x-ray optic for CAST is of a relatively small size, as only photons coming out of a 50 mm bore will be reflected and the focal length is limited to 1.5 m due to one of the side walls in the CAST building.

An already proven technology for building Wolter I type optics for space based applications is used in the NuSTAR telescope.[7,8] Slumped glass pieces, each 0.2 mm thick are placed on a SiC mandrel and graphite spacers are used to hold each piece in place at the correct angle. Two stacks of slumped glass substrates with graphite spacers are required for the double reflection geometry of the Wolter I optic. The optic for CAST will be made from spare NuSTAR glass, but only using 1/6th of the full circle and with an adjusted mandrel.

The angle of each glass substrate depends on the focal length, l, and radius, r, and is described as $\tan 4\alpha = r/l$. Every layer put on the mandrel has to have a width wide enough to cover the bore opening which sets a lower limit on the radius of the innermost glass layer. Each subsequent glass substrate is mounted on top of the earlier so there is no overlap. The resulting diagram for an optic optimized for a 50 mm bore opening and 1.5 m focal length is shown in figure 2.

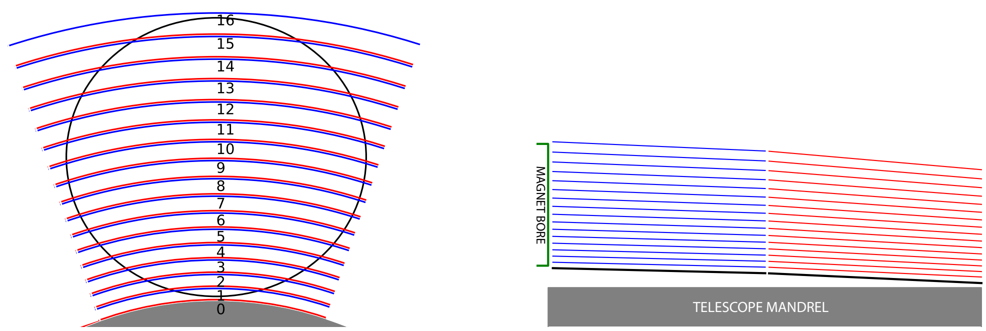

Figure 2. Diagrams of glass layering in Wolter I optic for the CAST axion helioscope. **Left:** Optic as seen from front. The circle shows the magnet bore opening compared to the optic. **Right:** Optic seen from side. Horizontal axis is compressed to show the tilt of each glass layer.

3. CAST COATINGS

Optimal coatings were calculated by taking into consideration detector efficiency, axion spectrum at each optical glass angle in the telescope. Axion spectrum is given by theory as a curve reminiscent of black body radiation between 0.1 and 10 keV as seen in figure 3.

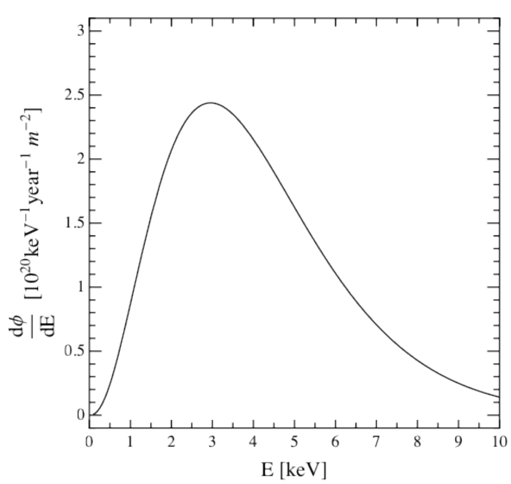

Figure 3. Solar axion flux spectrum at Earth, originating from the Primakoff process.

Material types investigated were multilayers of W/B_4C, W/Si, Pt/B_4C, Ni/B_4C as well as single layers of W, Pt, Ir and Ni. W/B4C and W/Si are well understood coatings for x-ray reflectivity and considerably less expensive to use W than Pt or Ir. Using B4C instead of Si as the light material will give increase reflectivity at 1 - 4 keV, but also gives slightly higher stress in the coating.[9] Ni/B4C coatings are not well understood and can give a high interfacial roughness between light and heavy material, but performs similar to W/B4C and Ir/B4C at 1-10 keV.

At a given glass substrate angle, α, the coating geometry was optimized by trying every combination in a parameter space of n (number of bilayers), d_{min} (minimum bilayer thickness), d_{max} (maximum bilayer thickness) and Γ (ratio between heavy and light material in a bilayer.) For every combination, the x-ray reflectivity was calculated using IMD[10] , multiplied with axion spectrum and detector effeciency and integrated to give a figure of merit (eqn. 1). The F.O.M. found in the parameter space is chosen as the optimal coating recipe for the given angle and focal length.

$$F.O.M. = \int_{0.1}^{10} R^2(\alpha, E)\ QE_{det}(E)\ S_{axion}\ dE \tag{1}$$

Output for optimized coating recipes for a w/B_4C material combination can be seen on the left side of figure 4. Each glass substrate layer should have between 2 and 6 bilayers with d-spacings between 50 and 260 Å.

A comparison of material combinations is seen on the right side og figure 4. The effective areas are calculated using eqn 2. Multilayers are seen to easily outperform the single layer coatings. Best performing are W/B_4C and Ni/B_4C multilayers.

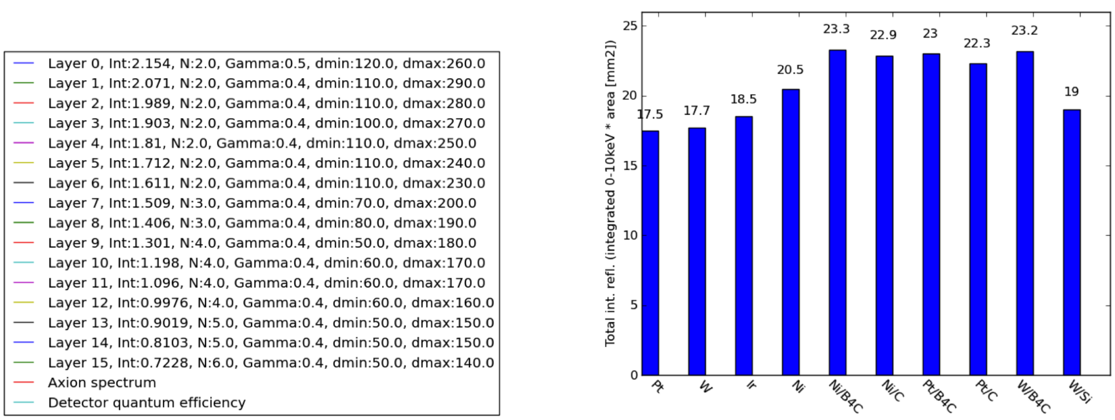

Figure 4. Results of multilayer coating optimization for the CAST Wolter I optic. **Left:** Optimized recipe for each layer in the optic. **Right:** Effective area comparison between each optimized material combination recipe.

$$A_{effective} = \sum_{i=1}^{N} \int_{0.1}^{10} R_i^2(\alpha, E)\ QE_{det}(E)\ S_{axion}\ A_i\ dE \tag{2}$$

4. TELESCOPES FOR THE IAXO HELIOSCOPE

A next generation axion helioscope currently in the proposal stage is the International AXion Observatory, IAXO.[11–13] It is a direct successor to CAST, with much larger magnet bores, bigger super conducting magnet and possibility of higher inclination, meaning it can measure axions coming from the sun 12 hours a day. An illustration can be seen in figure 5

Optimal coatings were calculated by taking into consideration detector efficiency, axion spectrum at each optical glass angle in the telescope. The telescope geometry, glass substrate angles and positions were first computed for focal lengths 4, 5, 6, 7, 8, 9 and 10 m. For each focal length, the x-ray reflectivity at 1-10 keV

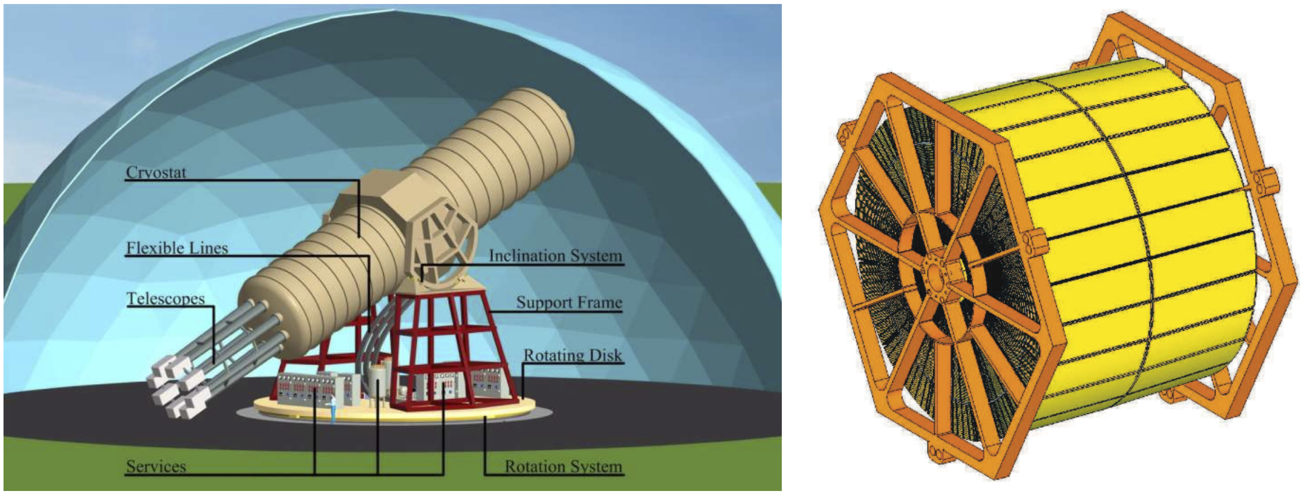

Figure 5. IAXO, a next generation axion helioscope. **Left:** Model of proposed IAXO setup. Superconducting magnet (cryostat) with 8 bores each 600 mm in diameter placed on a rotating platform to track the sun. **Right:** Model of a single Wolter I type optic for IAXO. One optic will be placed on the end of each bore.

for each coating material combination and thin film geometry were compared. Axion spectrum and detector efficiency were included in the comparison.

For a focal length of 4 m and bore diameter of 0.6 m, 110 glass substrate layers are needed to focus incoming x-rays to the same spot. At increasing focal length, even more glass layers and for 10 m focal length, required glass layers reach 235. To simplify the optimization and eventual coating deposition, the number of coating 'recipes' are fixed at 10, so only 10 different coatings will be required for a telescope.

5. IAXO TELESCOPE FOCAL LENGTH

To calculate the total telescope efficiency at a given focal length, the following equation was used.

$$\text{Throughput}_i = \frac{R_i^2 * A_{cs} * 0.8}{A_{bore}} \tag{3}$$

The fraction of photons reflected by layer i could be found using the cross sectional area of a layer opening and the total area of the bore opening. The factor 0.8 was used to include obscurations in the form of substrate spacers.

To find the optimal focal length, a non traditional approach was used. For a generic x-ray optic, the longer focal length gives a higher effective area, which was also the case here. But at increasing focal lengths, the focused spot also becomes bigger as a result of optic HPD (Half Power Diameter). Since the goal was to find a signal in the background, it was desirable to use a detector as small as possible, considering that the area of the detector is proportional to the background. In order to minimize detector area, it was therefore required to minimize the focused spot size, while also maximizing the effective area of the telescope. Spot area was determined using the enclosed energy diameter (EED) of the telescope at focal length f using a telescope HPD of 2 arc seconds for the worst case scenario and 1 arc second for the best case. EED of the sun (EED_{sun}) was also included using an HPD of 3.61 arc minutes. A combined EED of $(\text{EED}^2 + \text{EED}_{\text{sun}}^2)^{\frac{1}{2}}$ was used to calculate the area of the spot.

A new figure of merit, which also includes the square root of the spot arean was used for optic optimization:

$$F.O.M. = \frac{\int_{0.1}^{10} R^2(\alpha, E)\; QE_{det}(E)\; S_{axion}\; dE}{\sqrt{a}} \tag{4}$$

The parameter space used for optimization was identical to that used for the CAST optic, but with a variety of focal lengths from 4 m to 10 m and with only one material combination (W/B_4C). The result can be seen in figure 6. A notable difference in F.O.M. can be seen as focal length increases, resulting in larger focused spot. The optimal focal length is seen to be 5 m.

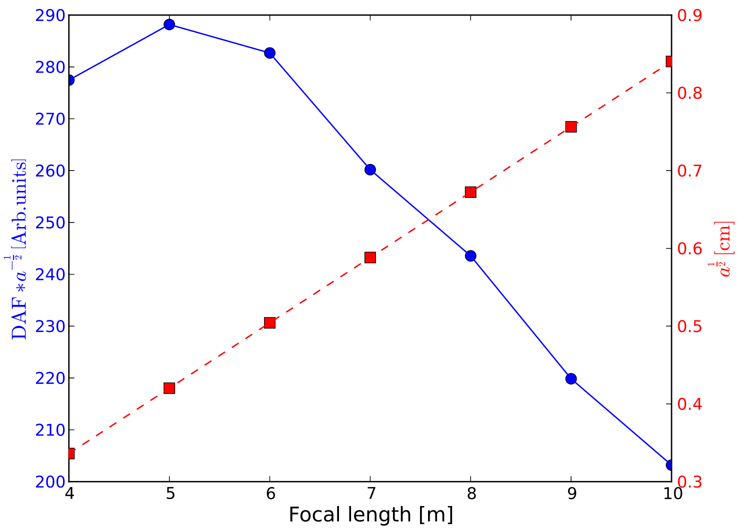

Figure 6. Result of focal length optimization. Circles show the throughput divided by the square root of the focused spot area. Squares show the square root of the focused spot area.

6. CONCLUSION

Software was developed to optimize geometry and multilayer coatings for the CAST axion helioscope. By including both detector quantum efficiency and axion spectrum in the optimizxation procedure, a true value of coating efficiency can be found. Maximum throughput can be achieved using either Ni/B_4C or W/B_4C multilayer coatings with 2-6 bilayers and d-spacings of 5-26 nm.

An extension of same software was used to find the optimal focal length of optics for the next generation IAXO axion helioscope. Using W/B_4C multilayer coatings and including the size of the focused spot in the calculations, a optimal focal length of 5 m was found.

REFERENCES

[1] Primakoff, H., "Photo-Production of Neutral Mesons in Nuclear Electric Fields and the Mean Life of the Neutral Meson," *Physical Review* **81**, 899–899 (Mar. 1951).

[2] Iguaz, F. J., "The CAST experiment: status and perspectives," *arXiv.org* (Oct. 2011).

[3] Ferrer-Ribas, E., Arik, M., Aune, S., Barth, K., Belov, A., Borghi, S., Bräuninger, H., Cantatore, G., Carmona, J. M., Cetin, S. A., Collar, J. I., Dafni, T., Davenport, M., Eleftheriadis, C., Elias, N., Ezer, C., Fanourakis, G., Friedrich, P., Galan, J., Garcia, J. A., Gardikiotis, A., Gazis, E. N., Geralis, T., Giomataris, I., Gninenko, S., Gomez, H., Gruber, E., Guthörl, T., Hartmann, R., Haug, F., Hasinoff, M. D., Hoffmann, D. H. H., Iguaz, F. J., Irastorza, I. G., Jacoby, J., Jakov vcić, K., Karuza, M., Königsmann, K., Kotthaus, R., Krcmar, M., Kuster, M., Lakic, B., Laurent, J. M., Liolios, A., Ljubičić, A., Lozza, V., Lutz, G., Luzon, G., Morales, J., Niinikoski, T., Nordt, A., Papaevangelou, T., Pivovaroff, M. J., Raffelt, G., Rashba, T., Riege, H., Rodriguez, A., Rosu, M., Ruz, J., Savvidis, I., Silva, P. S., Solanki, S. K., Stewart, L., Tomas, A., Tsagri, M., van Bibber, K., Vafeiadis, T., Villar, J., Vogel, J. K., Yildiz, S. C., and Zioutas, K., "Results and perspectives of the solar axion search with the CAST experiment," *arXiv.org* (Sept. 2012).

[4] Papaevangelou, T., "Status report of the CAST Experiment & Running in 2013-2014," Tech. Rep. CERN-SPSC-2012-028. SPSC-SR-106, Geneva (Oct. 2012).

[5] Barth, K., Belov, A., Beltran, B., Bräuninger, H., Carmona, J. M., Collar, J. I., Dafni, T., Davenport, M., Di Lella, L., Eleftheriadis, C., Englhauser, J., Fanourakis, G., Ribas, E. F., Fischer, H., Franz, J., Friedrich, P., Galan, J., Garcia, J. A., Geralis, T., Giomataris, I., Gninenko, S., Gomez, H., Hassinoff, M. D., Heinsius, F. H., Hoffmann, D. H. H., Irastorza, I. G., Jacoby, J., Jakovcic, K., Kang, D., Königsmann, K., Kotthaus, R., Kousouris, K., Krcmar, M., Kuster, M., Lakic, B., Liolios, A., Ljubičić, A., Lutz, G., Luzon, G., Miller, D. W., Papaevangelou, T., Pivovaroff, M. J., Raffelt, G., Redondo, J., Riege, H., Rodriguez, A., Ruz, J., Savvidis, I., Semertzidis, Y., Stewart, L., van Bibber, K., Vieira, J. D., Villar, J. A., Vogel, J. K., Walckiers, L., and Zioutas, K., "CAST constraints on the axion-electron coupling," *arXiv.org* (Feb. 2013).

[6] Tomas, A., Ferrer-Ribas, E., Luzon, G., Gomez, H., Ruz, J., Dafni, T., Segui, L., Fanourakis, G., Yildiz, S. C., Galan, J., Giomataris, I., Aune, S., Geralis, T., Gardikiotis, A., Morales, J., Iguaz, F. J., Garcia, J. A., Rodriguez, A., Papaevangelou, T., Irastorza, I. G., and Vafeiadis, T., "The new micromegas X-ray detectors in CAST," *X-Ray Spectrom.* **40**(4), 240–246 (2011).

[7] Harrison, F. A., Craig, W. W., Christensen, F. E., Hailey, C. J., Zhang, W. W., Boggs, S. E., Stern, D., Cook, W. R., Forster, K., Giommi, P., Grefenstette, B. W., Kim, Y., Kitaguchi, T., Koglin, J. E., Madsen, K. K., Mao, P. H., Miyasaka, H., Mori, K., Perri, M., Pivovaroff, M. J., Puccetti, S., Rana, V. R., Westergaard, N. J., Willis, J., Zoglauer, A., An, H., Bachetti, M., Barrière, N. M., Bellm, E. C., Bhalerao, V., Brejnholt, N. F., Fuerst, F., Liebe, C. C., Markwardt, C. B., Nynka, M., Vogel, J. K., Walton, D. J., Wik, D. R., Alexander, D. M., Cominsky, L. R., Hornschemeier, A. E., Hornstrup, A., Kaspi, V. M., Madejski, G. M., Matt, G., Molendi, S., Smith, D. M., Tomsick, J. A., Ajello, M., Ballantyne, D. R., Baloković, M., Barret, D., Bauer, F. E., Blandford, R. D., Brandt, W. N., Brenneman, L. W., Chiang, J., Chakrabarty, D., Chenevez, J., Comastri, A., Dufour, F., Elvis, M., Fabian, A. C., Farrah, D., Fryer, C. L., Gotthelf, E. V., Grindlay, J. E., Helfand, D. J., Krivonos, R., Meier, D. L., Miller, J. M., Natalucci, L., Ogle, P., Ofek, E. O., Ptak, A., Reynolds, S. P., Rigby, J. R., Tagliaferri, G., Thorsett, S. E., Treister, E., and Urry, C. M., "THE NUCLEAR SPECTROSCOPIC TELESCOPE ARRAY(NuSTAR) HIGH-ENERGY X-RAY MISSION," *The Astrophysical Journal* **770**, 103 (May 2013).

[8] Christensen, F. E., Jakobsen, A. C., Brejnholt, N. F., Madsen, K. K., Hornstrup, A., Westergaard, N. J., Momberg, J., Koglin, J., Fabricant, A. M., Stern, M., Craig, W. W., Pivovaroff, M. J., and Windt, D., "Coatings for the NuSTAR mission," in [*SPIE Optical Engineering + Applications*], O'Dell, S. L. and Pareschi, G., eds., 81470U–81470U–19, SPIE (Sept. 2011).

[9] Jakobsen, A. C., Ferreira, D. D. M., Christensen, F. E., Shortt, B., Collon, M., and Ackermann, M. D., "Preliminary coating design and coating developments for ATHENA," in [*Optics for EUV, X-Ray, and Gamma-Ray Astronomy V*], 81470T–8, SPIE (Sept. 2011).

[10] Windt, D. L., "IMD—Software for modeling the optical properties of multilayer films," *Computers in Physics* **12**, 360 (1998).

[11] Irastorza, I. G., Avignone, F. T., Caspi, S., Carmona, J. M., Dafni, T., Davenport, M., Dudarev, A., Fanourakis, G., Ferrer-Ribas, E., Galan, J., Garcia, J. A., Geralis, T., Giomataris, I., Gomez, H., Hoffmann, D. H. H., Iguaz, F. J., Jakovcic, K., Krcmar, M., Lakic, B., Luzon, G., Pivovaroff, M., Papaevangelou, T., Raffelt, G., Redondo, J., Rodriguez, A., Russenschuck, S., Ruz, J., Shilon, I., Ten Kate, H., Tomas, A., Troitsky, S., van Bibber, K., Villar, J. A., Vogel, J., Walckiers, L., and Zioutas, K., "Towards a new generation axion helioscope," *arXiv.org* (Mar. 2011).

[12] Irastorza, I. G., Avignone, F. T., Cantatore, G., Caspi, S., Carmona, J. M., Dafni, T., Davenport, M., Dudarev, A., Fanourakis, G., Ferrer-Ribas, E., Galan, J., Garcia, J. A., Geralis, T., Giomataris, I., Gninenko, S., Gomez, H., Hoffmann, D. H. H., Iguaz, F. J., Jakovcic, K., Krcmar, M., Lakic, B., Luzon, G., Lindner, A., Pivovaroff, M., Papaevangelou, T., Raffelt, G., Redondo, J., Russenschuck, S., Ruz, J., Shilon, I., Ten Kate, H., Tomas, A., Troitsky, S., van Bibber, K., Villar, J. A., Vogel, J., Walckiers, L., and Zioutas, K., "The International Axion Observatory (IAXO)," *arXiv.org* (Jan. 2012).

[13] Vogel, J. K., Avignone, F. T., Cantatore, G., Carmona, J. M., Caspi, S., Cetin, S. A., Christensen, F. E., Dael, A., Dafni, T., Davenport, M., Derbin, A. V., Desch, K., Diago, A., Dudarev, A., Eleftheriadis, C., Fanourakis, G., Ferrer-Ribas, E., Galan, J., Garcia, J. A., Garza, J. G., Geralis, T., Gimeno, B., Giomataris, I., Gninenko, S., Gomez, H., Hailey, C. J., Hiramatsu, T., Hoffmann, D. H. H., Iguaz, F. J., Irastorza, I. G.,

Isern, J., Jaeckel, J., Jakovcic, K., Kaminski, J., Kawasaki, M., Krcmar, M., Krieger, C., Lakic, B., Lindner, A., Liolios, A., Luzon, G., Ortega, I., Papaevangelou, T., Pivovaroff, M. J., Raffelt, G., Redondo, J., Ringwald, A., Russenschuck, S., Ruz, J., Saikawa, K., Savvidis, I., Sekiguchi, T., Shilon, I., Silva, H., ten Kate, H. H. J., Tomas, A., Troitsky, S., van Bibber, K., Vedrine, P., Villar, J. A., Walckiers, L., Wester, W., Yildiz, S. C., and Zioutas, K., "IAXO - The International Axion Observatory," *arXiv.org* (Feb. 2013).